Möller, A., Nordheim, A., Kozlowski, S. A., Patel, D. J., & Rich, A. (1984) *Biochemistry 23*, 54-62.
Nandi, S., Wang, J. C., & Davidson, N. (1965) *Biochemistry 4*, 1687-1696.
Omenn, G. S., Cuatrecasas, P., & Anfinsen, C. B. (1969) *Proc. Natl. Acad. Sci. U.S.A. 64*, 923-930.
Rich, A., Nordheim, A., & Wang, A. H.-J. (1984) *Annu. Rev. Biochem. 53*, 791-846.
Simpson, R. B. (1964) *J. Am. Chem. Soc. 86*, 2059-2065.
The Worthington Manual (Enzymes and Related Biochemicals) (1988) pp 229-232, Worthington Biochemical Corp., Freehold, NJ.
Thomas, C. A. (1954) *J. Am. Chem. Soc. 76*, 6032-6034.
Tunis-Schneider, M. J. B., & Maestre, M. F. (1970) *J. Mol. Biol. 52*, 521-541.
von Hippel, P. H., & Felsenfeld, G. (1964) *Biochemistry 3*, 27-39.
Yamane, T., & Davidson, N. (1961) *J. Am. Chem. Soc. 83*, 2599-2607.
Zacharias, W., Larson, J. E., Klysik, J., Stirdivant, S. M., & Wells, R. D. (1982) *J. Biol. Chem. 257*, 2775-2782.

Sequence Specificity of the Deoxyribonuclease Activity of 1,10-Phenanthroline–Copper Ion†

Chun Yoon,‡ Michio D. Kuwabara,‡ Annick Spassky,§ and David S. Sigman*,‡
Department of Biological Chemistry, School of Medicine, Department of Chemistry and Biochemistry, and Molecular Biology Institute, University of California, Los Angeles, California 90024, and Institut Pasteur, 75724 Paris Cedex 15, France
Received June 14, 1989; Revised Manuscript Received October 9, 1989

ABSTRACT: A statistical analysis of a data set composed of over 1600 scission events of DNA produced by the 2:1 1,10-phenanthroline–copper complex (OP–Cu) has demonstrated that the nucleotide 5′ to the site of phosphodiester bond scission is a primary influence in the kinetics of cleavage at any sequence position. The scission was less affected by the 3′ neighbor. For each of the sixteen possible dinucleotides, a kinetic parameter can be computed reflecting scission at the 3′ nucleotide. When used to predict the scission pattern of a DNA sequence not part of the present data set, correlation coefficients of about 0.6 between predicted and observed patterns were obtained.

The nuclease activity of 1,10-phenanthroline–copper (OP–Cu)[1] exhibits sequence specificity in its efficient scission of B-DNA although it oxidizes the deoxyriboses of all four bases (Sigman, 1986). The major reaction pathway of the nuclease activity is summarized in Figure 1 and has been supported by the isolation of the free bases, 3′ and 5′ phosphomonoester termini, and 5-methylenefuranone (Pope et al., 1982; Kuwabara et al., 1986; Goyne & Sigman, 1987). In addition, by use of 5′-labeled DNA, a reaction intermediate has been trapped which likely corresponds to the reaction intermediate C (Kuwabara et al., 1986; Veal & Rill, 1989). The chemistry of the cleavage reaction demands that the coordination complex attack the deoxyribose from the minor groove.

The sequence-dependent scission of B-DNA and the specificity of the reaction for secondary structure can be attributed to a kinetic scheme in which the reaction is funnelled through an essential noncovalent intermediate [$(OP)_2Cu^+$–DNA] (Sigman et al., 1979; Thederahn et al., 1989).

$$(OP)_2Cu^+ + DNA \overset{K_d}{\leftrightarrow} (OP)_2Cu^+\text{–}DNA \xrightarrow{H_2O_2} \text{nicked products} \quad (1)$$

Preferred sites of scission are adjacent to high-affinity binding sites for the coordination complex within the minor groove. The specific interactions between the DNA and the coordination complex which result in tight binding in the minor groove have not been identified, but certain features of the sequence preference have been investigated. For example, the scission rates for a given sequence are insensitive to the length of the DNA fragment (Yoon et al., 1988a); repetitive sequences within a fragment exhibit comparable digestion patterns (Law et al., 1987). Tri- and tetranucleotide sequences have been identified which are preferentially cut. Veal and Rill (1988, 1989) have found that the central A of TAT is strongly cleaved and that related sequences such as TGT, TAAT, TAG, TAG–pyrimidine, and CAGT are moderately preferred. The most strongly cut sequence within the Tyr T promoter is CATATC (Drew & Travers, 1984). Sequences composed of A·T stretches are preferentially cleaved (Suggs & Wagner, 1986).

In this paper, we summarize our attempts to develop a statistical approach to the analysis of the sequence-dependent reactivity of OP–Cu. The most important variable influencing scission rates is the nucleotide 5′ to the site of scission.

Experimental Procedures

Methods

Reaction Conditions for OP–Cu Scission. Uniquely labeled restriction fragments were digested as previously described (Kuwabara et al., 1986; Kuwabara & Sigman, 1987). All sequencing gels were calibrated with the G+A reaction (Maxam & Gilbert, 1980).

† This research was supported by USPHS Grant GM 21199.
* Address correspondence to this author at the Molecular Biology Institute, University of California, Los Angeles, CA 90024.
‡ University of California.
§ Institut Pasteur.

[1] Abbreviations: OP–Cu, 2:1, 1,10-phenanthroline–copper complex; EDTA, ethylenediaminetetraacetic acid; MPE, methidiumpropyl-EDTA; DTT, dithiothreitol; bp, base pair; SD, standard deviation; Tris, tris(hydroxymethyl)aminomethane; PMA, phorbol 12-myristate 13-acetate.

0006-2960/90/0429-2116$02.50/0

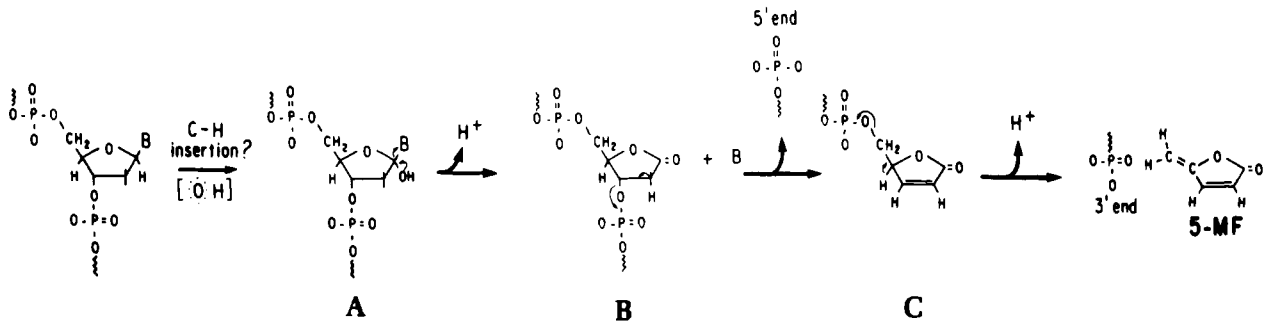

FIGURE 1: Proposed mechanism for scission of DNA by OP–Cu [from Goyne and Sigman (1987)].

Gel Retardation/OP–Cu Footprinting. Nuclear extracts were derived from the pre B cell 70Z/3 following treatment with PMA (Gaynor et al., 1988). Gel retardation/OP–Cu footprinting was carried out on entire gels as previously described except that OP–Cu reaction times were 15 min in the presence of 50 mM NaCl (Kuwabara & Sigman, 1987). After gel elution, DNA samples were phenol–chloroform and chloroform extracted before ethanol precipitation.

Data Analysis

A total of 1646 bases from various DNA fragments were analyzed. This number was comprised of 362 G's, 376 C's, 479 A's, and 429 T's. Although only digestion patterns derived from double-helical DNA were analyzed, the G:C and A:T ratio deivated from 1 because complementary strands were analyzed separately. These sequences included the *lac* promoter and operator region fragments from both wild-type and UV-5 mutant sequences (Yoon et al., 1988a), the HIV enhancer and long terminal repeat regions (Gaynor et al., 1988), the immunoglobulin κ gene enhancer region (Gaynor et al., 1988), the trp EDCBA promoter fragment (Chen & Sigman, 1987), and the mouse immunoglobulin heavy chain μ_m sequence (Law et al., 1987). Data from polyacrylamide gel separation of cleaved fragments were collected on both an L-1000 drum scanner (Optronics Int.) and an LKB Model 2222-010 densitometer (Pharmacia LKB Biotechnology, Inc.). Gel density integration and subsequent rate constant calculations were performed as described. We were able to accurately integrate between 45 to 85 peaks per gel.

Expected Value Calculations. Expected values for propensity of OP–Cu cleavage were calculated in the following manner. For each gel sequence, first-order rate constants were calculated for each residue and then segregated into quartiles of equal size with the fastest rates grouped into the first quartile and the slowest rates assigned to the fourth quartile. For analysis with oligonucleotide templates, the segregating variable was the rate constant at one of the residues within the template rather than the average for the group. After all residues were segregated and scored, expected value calculations were performed by using the equation:

$$EV = \sum_{i=1}^{4} (\%\ \text{in quartile}_i)[100 - 33.3(i - 1)]$$

A randomly cleaved nucleotide will have an EV = 50. Nucleotides which are well cleaved usually fall into the first or second quartiles and therefore have an EV >50. A poorly cleaved nucleotide will have an EV <50 because most of its rate constants will fall into the third and fourth quartiles. Expected values for cleavage propensities were originally calculated separately for data collected from each instrument, but given their near-identical results, the data sets were merged together and the reported expected values are from the merged data set.

Random Distribution of Nucleotides. In a densitometer tracing of a gel, the density of a band is, in part, observed to be a function of its length of migration. This artifact is minimized if the distribution of each of the four nucleotides is random; i.e., all nucleotides are distributed equally along the length of each analyzed DNA sequence when all the sequences are averaged together. We define an index, IR, to check that this is the case. IR is given by the equation:

$$IR_i = \frac{\sum_{\text{gels}} (\text{position of } i)/(\text{length of gel})}{\text{total no. of } i}$$

i is each of the four nucleotides. Equal distribution of the four nucleotides will result in equal values for IR. For all the sequences analyzed during this study, the IR indices for each nucleotide were A = 0.48, T = 0.52, G = 0.53, and C = 0.51. The similarity in all these values suggests that positional artifact is not likely to be a major contributor to variations seen in the calculated expected values for OP–Cu cleavage efficiency.

Results

NF-κB Binding Site. (A) Analysis of DNA Conformation. Repetitive sequences from the region of transcription termination of the μ_m immunoglobulin gene exhibit pronounced similarity in their OP–Cu scission pattern near the 3′ end of each strand but variability near the 5′ terminus (Law et al., 1987). The influence of neighboring nucleotides on the scission pattern of repetitive sequences was investigated further by using the 10 bp DNA sequence which binds the enhancer protein NF-κB that is essential for the B cell specific expression of the κ light chain gene (Sen & Baltimore, 1986, 1987). This DNA sequence is present twice in the HIV LTR and is essential for the maintenance of HIV infectivity (Nabel & Baltimore, 1987). The identity of the two HIV sequences is restricted to a 10 bp identity. However, each HIV sequence shares an 11 bp identity with the κ enhancer sequence (see legend to Figure 2).

Both strands of the three copies of the NF-κB binding sites were digested with OP–Cu (Figure 2). The cleavage rate constants for the κ enhancer sequence correlate extremely well with the cleavage pattern of both HIV sequences over their 11 bp identities (see Table I, where $r = 0.98$ and $r = 0.99$ for the κ enhancer and the first and second HIV enhancer repeats, respectively). The correlation coefficient between cleavage rate constants for the 10 bp NF-κB binding site is markedly higher than the correlation coefficient between cleavage rate constants for a 16 bp stretch of DNA which includes the 10 bp repeat sequence at its center ($r = 0.97$ versus $r = 0.14$). When discrepancies exist between cleavage rate constants of identical sequences nested in different flanking sequences, they occur at the first two bases at the 5′ end of the identical sequence. These results suggest that nucleotides 5′ to the

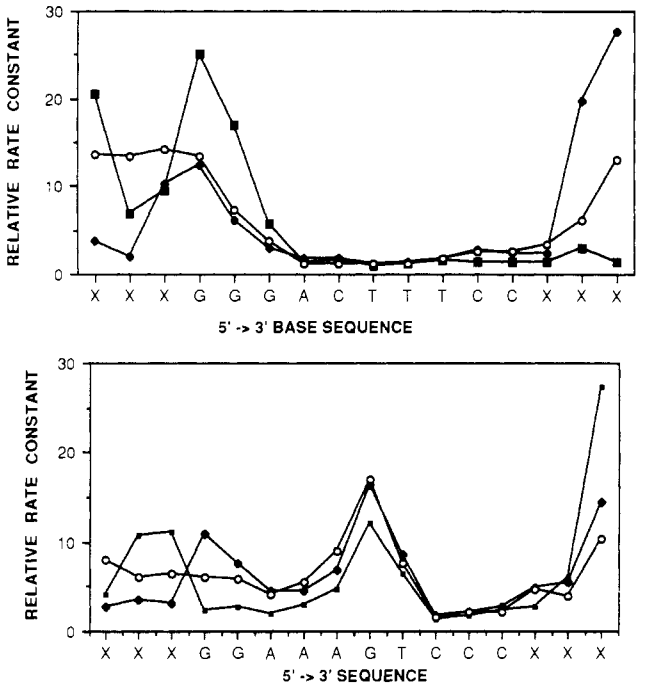

FIGURE 2: Relative first-order rate constants for OP–Cu cleavage of NF-κB binding domains and flanking regions in the HIV and κ light chain enhancer DNA fragment.

5′-CAAGGGACTTTCCGCT-3′
3′-GTTCCCTGAAAGGCGA-5′
(■) distal NF-κB binding site of HIV LTR
positions −108 to −98

5′-CTGGGGACTTTCCAGG-3′
3′-GACCCCTGAAAGGTCC-5′
(♦) proximal NF-κB binding site of HIV LTR
positions −94 to −79

5′-GAGGGGACTTTCCGAG-3′
3′-CTCCCCTGAAAGGCTC-5′
(○) NF-κB binding site of κ light chain enhancer

Table I: Correlation Coefficients between OP–Cu Cleavage Rate Constants of the 5′-Labeled Top (Nontemplate Strand) of NF-κB Recognition and Flanking Sequences[a]

sequence 1 vs	sequence 2	no. of bases	*R*
HIV, −108 to −98	HIV, −94 to −79	10	0.97
HIV, −108 to −98	HIV, −97 to −79	16	0.14
HIV, −108 to −98	κ enhancer	11	0.97
HIU, −108 to −98	κ enhancer	16	0.67
HIV, −94 to −79	κ enhancer	11	0.98
HIV, −94 to −79	κ enhancer	16	0.54

[a] See legend of Figure 1 for sequences.

scission site strongly influence the cleavage rate.

(B) Binding of Enhancer Protein to Two Closely Related Sites. The protein binding affinities of the proximal NF-κB site of HIV LTR and the κ light chain were compared to determine if functional differences were associated with altered OP–Cu scissions rates. By carrying out OP–Cu footprinting following gel retardation (Kuwabara & Sigman, 1987), it was possible to show that the enhancer protein binds more tightly to the recognition sequence in the κ light chain enhancer than to the proximal HIV enhancer sequence in 50 mM NaCl. In 50 mM Tris buffer without added NaCl, both sequences bind the protein with equivalent affinity. Protein was partially purified from nuclear extracts derived from PMA-treated HeLa cells (Gaynor et al., 1988).

Statistical Analysis. (A) Dinucleotide Template Analysis. Although the cleavage reaction proceeds at all nucleotides, OP–Cu exhibits a measurable preference for cleavage at guanosine [expected value (EV) = 62.5], slower rates at cytosines (EV = 36.7), and average rates of cleavage at adenosines (EV = 47.5) and thymidines (EV = 47). The scission events of 1646 nucleotides were analyzed at each nucleotide in which the nucleotide was either the 3′ or 5′ nucleotide of one of the 16 possible dinucleotide pairs. When the expected values are calculated on the basis of the cleavage rates of the 5′ nucleotide in a dinucleotide pair, we find that there is fairly uniform cleavage of all dinucleotides with the exception of the poorly cleaved combinations (5′ → 3′) C-C, A-A, and T-C and the very well cleaved combinations G-T and T-A (Figure 3). The mean expected value for all 16 possible dinucleotide combinations is 49.2 with a standard deviation of 13.6. When we calculate expected values for cleavage based on the OP–Cu scission of the 3′ nucleotide of a dinucleotide, the mean expected value for all possible combinations remains unchanged at 49.2, but the SD increases to 21.6 (Figure 3). The increased variance suggest that the 5′ nucleotide influences OP–Cu cleavage efficiency of its 3′ neighbor more than the 3′ nucleotide affects OP–Cu cleavage of its 5′ neighbor.

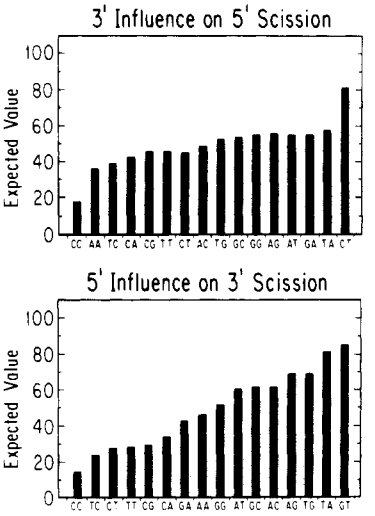

FIGURE 3: Bar graph representation of expected values for dinucleotides.

Interesting results from the statistical analysis of the 5′ nucleotide on scission are as follows: (a) the high efficiency of G-T and T-A templates despite the equivalent expected values of scission for adenosines and thymidines calculated without regard to the 5′ nucleotide; (b) a consistent decrease in OP–Cu cleavage rates for any nucleotide which has a cytosine as its 5′ neighbor; (c) the decreased propensity of cleavage of homopyrimidines TT, CC, TC, and CT especially at the 3′ nucleotide; and (d) the higher cleavage efficiency of all alternating dinucleotides R-Y and Y-R (Y, pyrimidine; R, purine) with the expection of those purines with a 5′ cytosine. There is no consistent inhibition or enhancement of cleavage of purine homopolymer R-R steps. It appears that the geometry of purine/pyrimidine alternating sequences is conducive for OP–Cu binding and cleavage, while pyrimidine dimers tend to inhibit OP–Cu cleavage.

(B) Purine/Pyrimidine Multinucleotide Template Analysis. Expected value calculations of OP–Cu cleavage propensities of trinucleotide templates cannot be calculated because of the limited data set. However, tri- and tetranucleotides can be analyzed as sequences of purines and pyrmidines. The expected values for OP–Cu cleavage of purines and pyrimidines individually are 54.0 and 42.7, respectively. The increased tendency for purine cleavage is attributable to OP–Cu preference for guanines, while the decreased cleavage of pyrimidines is due to the poor cleavage of cytosine.

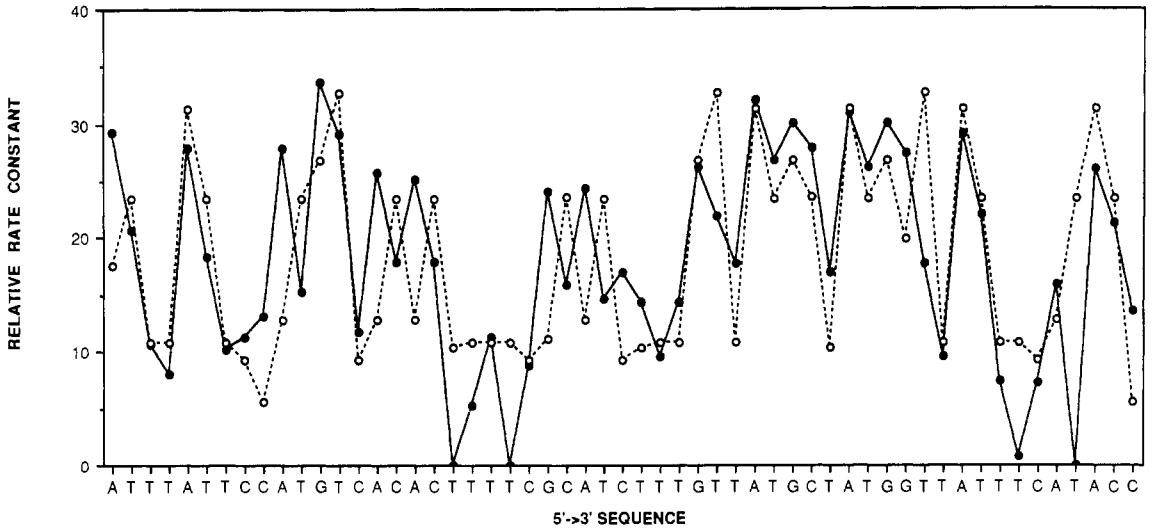

FIGURE 4: Observed and predicted OP–Cu scission of the *gal* operon DNA fragment. Open circles = expected cleavage; closed circles = observed cleavage rates.

Tetranucleotide templates based on cleavage rates of the first nucleotide in the template (see Table II, column 2) indicate that the sequences least likely to be cleaved are -YYYY-, -YYYR-, and -YYRY- (5′ → 3′). Examination of scission rates of the second, third, and fourth nucleotides within tetranucleotides indicates that pyrimidine dimers are poorly cleaved at the 3′ nucleotide and that alternating purine/pyrimidine (R-Y) dimers are well cleaved. Hence, in Table II, column 3, all sequences with -YYNN- are poorly cleaved while the sequences -RYNN- reveal an enhanced propensity for scission. In column 4, sequences -NYYN- are poorly cleaved while sequences -NRYN- are well cleaved. Finally, in column 5, the sequences -NNYY- have low expected values for cleavage while the sequences -NNRY- have higher expected values. The triplet sequences, which have the highest expected values of OP–Cu cleavage in both column 4 (-YRYN-) and column 5 (-NYRY-), suggest that a 3′ base alternating sequence further enhances OP–Cu oxidative efficiency. Y-R sequences do not show enhanced scission in the tetranucleotide template analysis because of the conflicting tendencies of C and T. In the dinucleotide templates, thymines 5′ to purines increase their expected value for cleavage above that for purines alone, but the presence of cytosines positioned 5′ to purines significantly decreases the expected value of cleavage.

The tetranucleotide analysis further supports the hypothesis that the dinucleotide unit is the major determinant of OP–Cu cleavage. Comparison of the mean and standard deviations of each column of Table II reveals little variation in the mean expected value. However, columns 3–5 have a higher standard deviation than column 2. This implies that the 5′ nucleotides affect OP–Cu scission at their 3′ neighbors more than 3′ nucleotides affect their 5′ neighbors' cleavage.

(*C*) *Predicting OP–Cu Cleavage Patterns.* One use for the dinucleotide template and the tetranucleotide purine/pyrimidine template cleavage analyses is to predict OP–Cu scission patterns. Correlation coefficients were calculated between the observed OP–Cu cleavage of the DNA restriction fragments in our data base and predicted OP–Cu cleavage by using the expected values from the dinucleotide template analyses. A marked difference is seen when correlation coefficients are determined on the basis of cleavage at the 5′ nucleotide of the dinucleotide template as compared to those based on OP–Cu cleavage at the 3′ nucleotide. For expected values from OP–Cu oxidation of the 3′ nucleotide, the correlation coefficients ranged from a low of $r = 0.59$ to a high of $r = 0.74$. Correlation coefficients from expected values of OP–Cu cleavage at the 5′ nucleotide were consistently less than $r = 0.50$. Using the expected values of cleavage from tetranucleotide templates, the correlation coefficients between observed and predicted cleavage did not exceed $r = 0.6$ for any gel, irrespective of the position in the template used as the segregating variable.

Table II: Expected Value Calculations for OP–Cu Cleavage of Tetranucleotide Templates[a]

	4 base 1	4 base 2	4 base 3	4 base 4
RRRR	54.37	49.21	46.43	57.54
YRRR	62.78	54.44	52.78	45.56
RYRR	66.67	70.18	56.73	58.77
YYRR	44.98	27.71	46.59	56.63
RRYR	53.70	61.11	67.41	55.56
YRYR	42.99	59.50	74.45	66.67
RYYR	62.87	68.35	30.38	62.03
YYYR	34.63	18.45	23.30	42.39
RRRY	45.30	46.44	59.54	55.27
YRRY	36.84	45.18	64.47	69.30
RYRY	51.37	70.98	68.24	81.96
YYRY	35.64	26.07	55.12	69.97
RRYY	38.30	60.64	54.26	13.83
YRYY	48.95	62.87	75.53	37.13
RYYY	59.38	59.38	19.10	11.46
YYYY	34.31	15.57	12.65	20.44
mean	48.32	49.76	50.44	50.28
SD	10.89	18.38	19.58	20.59

[a] Templates are based on purine (R) and pyrimidine (Y) composition. Column 2 = EV calculated from OP–Cu oxidation of the 5′ residue of the tetranucleotide template. Column 3 = EV calculated from OP–Cu oxidation of the second residue in the template. Column 4 = EV calculated from OP–Cu oxidation of the third residue in the template. Column 5 = EV calculated from OP–Cu oxidation of the 3′ residue of the template.

As a further test, the expected value data from dinucleotide templates cleaved at the 3′ residue were used to predict the scission pattern of a *gal* operon fragment (Spassky et al., 1988) which had not been previously incorporated into the data base. A comparison of the observed and predicted first-order rate constants is shown in Figure 4. The correlation coefficient obtained was 0.64. There is general agreement between the observed and predicted scission rates although occasional regions of incongruity are evident.

(*D*) *Correlation of Cleavage Preferences with DNA Helical Parameters.* Since local sequence affects OP–Cu cleavage of DNA, a search for possible correlations between the first-order rate constants of cleavage and the four DNA helix parameters

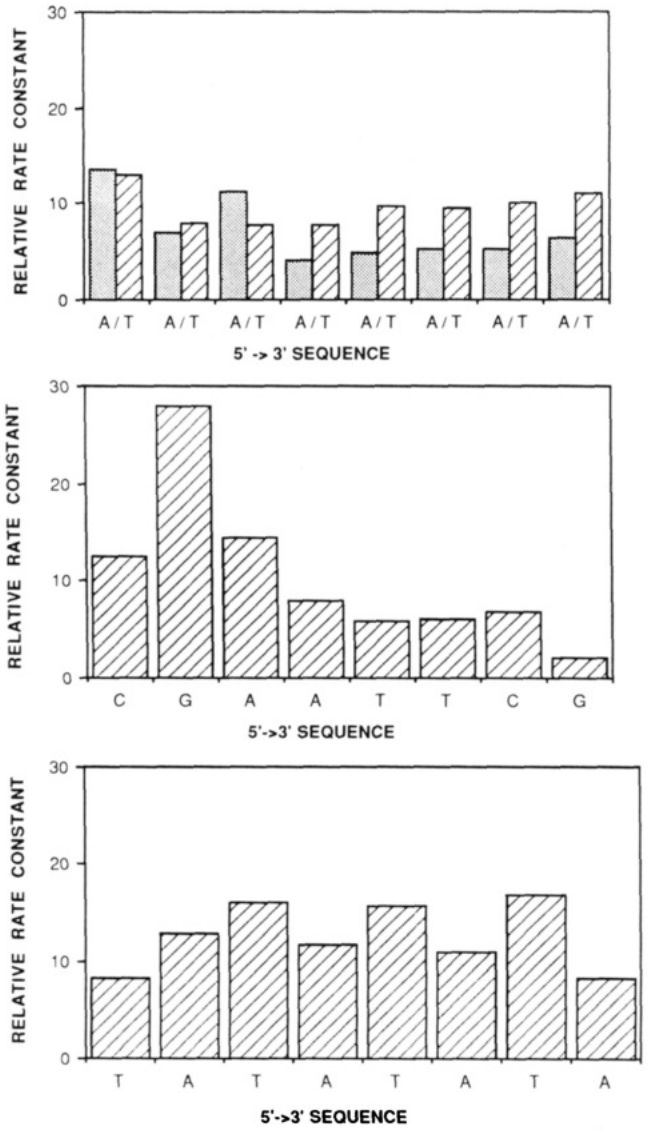

FIGURE 5: First-order rate constants for OP–Cu cleavage of dodecamers. Top: 5′-CGAAAAAAAACG-3′ (stippled); 5′-CGTTTTTTTTCG-3′ (hatched). Middle: 5′-CGCGAATTCGCG-3′. Bottom: 5′-CGTATATATACG-3′.

derived from the treatments of Calladine (1982) and Dickerson (1983) was conducted. Helix parameters for the dodecamer CGCGAATTCGCG, whose X-ray structure is known (Drew & Dickerson, 1981a,b), were calculated and compared to the observed cleavage pattern of the same dodecamer. The parameters studied included the helix twist angle, base role angle, propeller twist, and the δ torsion angle. No statistically significant correlation between the helix parameters and the OP–Cu digestion pattern was obtained. Replacing the calculated helical parameters with the observed values from the X-ray crystallographic structure also failed to demonstrate any correlations by univariate or multivariate linear regression. The lack of significant correlations suggests that OP–Cu does not recognize a single helix parameter as defined above nor a linear combination of the four parameters.

(*E*) *OP–Cu Cleavage of Other Dodecamers*. Three other dodecamers were cleaved under the same conditions used for cleavage of the original dodecamer. The cleavage patterns of the central 8 bp of all the docecamers are presented in Figure 5. The homopolymer-containing sequences CGAAAAAAAACG and CGTTTTTTTTCG reveal slightly variable cleavage of the first three adenines of the former sequence and the first thymine of the latter sequence. However, the remainder of the homopolymer region is uniformly cleaved by OP–Cu.

OP–Cu scission of the alternating sequence CGTATATATACG reveals an obvious preference in cleavage of the thymines as compared to adenines. This occurs despite the neutral cleavage preference of OP-Cu observed for adenines and thymines from random sequence DNA.

Statistical analyses were carried out for all dodecamer sequences with predicted helix parameters from Dickerson (1983). Regression analysis for OP–Cu cleavage of the homopolymer sequences CGAAAAAAAACG and CGTTTTTTTTCG does show correlations between their cleavage pattern and predicted helix parameters but not with the CGCGAATTCGCG and CGTATATATACG dodecamers. The observed correlation for the homopolymer sequences results from their uniform cleavage by OP–Cu and their unvarying predicted helix parameters in their central regions. Crystallographic data are not yet available for the oligonucleotide sequences other than CGCGAATTCGCG.

Discussion

A statistical analysis of a data set composed of over 1600 base scission events produced by OP–Cu has demonstrated that the nucleotide 5′ to the site of phosphodiester bond scission is a primary influence in the kinetics of scission at any sequence position. The scission was less influenced by the 3′ neighbor. The statistical analysis based on the dinucleotide template provides an approach for predicting scission rates given the primary sequence. Using the data based on the dinucleotides alone, it is possible to obtain correlation coefficients of about 0.6 between predicted and observed scission patterns.

The predictability is not improved by using the tetranucleotide template of purines and pyrimidines. However, it should be improved when an enhanced data set allows calculation of expected values for specific tri- and tetranucleotides. These data will reflect the influence of the 3′ nucleotide as well as the modulation of a 5′ nucleotide beyond a single sequence position. The latter effect was apparent from studies of the scission of different Pribnow box sequences of the *lac* promoter. In this work, a mutational change at −9 had a major effect on the scission at −10, yet a base change at −8 also influenced cutting at −10, although to a lesser extent (Sigman et al., 1985; Spassky & Sigman, 1985).

The present analysis differs from previous studies of the specificity of OP–Cu which focused on identifying tri- and tetranucleotide sequences with clear preferred sites of scission in different DNA fragments (Cartwright & Elgin, 1982; Suggs & Wagner, 1986; Flick et al., 1986; Veal & Rill, 1988, 1989). These approaches underscore the importance of sequence determinants other than the 5′ nucleotide in determining scission efficiency. Nevertheless, although the cleavage propensities of OP–Cu in these studies were based on three or more nucleotides, there is good overall agreement with the current analysis. For example, the dinucleotide template predicts the scission pattern of the undecamer, 5′-CCCTTATCCCC-3′ (Veal & Rill, 1989). Prominent scission occurs at adenosine and thymidine of the T-A and A-T steps, respectively. The homopyrimidine step reveal decreased cleavage as would be expected from the dinucleotide analysis.

The preferred cutting at T relative to A in the deoxyoligonucleotide CGCTATATAGCG is not predicted by the expected values of the dinucleotide template summarized in Figure 3, in which a TA sequence is cleaved slightly more efficiently than an AT sequence. A possible explanation for this discrepancy is that the expected values were calculated from random sequence DNA and the alternating d-AT se-

quence, which is favored substrate of OP–Cu, exists in a modified B secondary structure (Scheffler et al., 1968; Klug et al., 1979; Yoon et al., 1988b). If it becomes possible to predict the scission pattern of random sequence DNA with confidence, disagreement in observed and predicted scissions rates may provide evidence for a systematic deviation from B-structure DNA.

Presently, it is not possible to infer the structural features of DNA which govern the cleavage patterns. Since substitution of an inosine for a guanosine enhances the rate of scission of a synthetic oligonucleotide (Veal & Rill, 1989), the 2-amino group clearly influences the binding of the coordination complex within the minor groove. However, this information is not sufficient to provide a clear picture of the reactive complex. Since there is variation in rates of scission of CGTATATATACG even though the minor groove width is constant (Yoon et al., 1988b), this structural feature also cannot be solely responsible for the observed variation in cleavage. No known or predicted structural parameter of DNA determined by X-ray crystallography of synthetic deoxyoligonucleotides correlates with the observed cleavage intensities. Determining the factors that govern OP–Cu cleavage specificity will provide insight into not only the origin of structural variability but also its role in modulating the interaction of a DNA sequence with binding proteins.

Registry No. OP–Cu, 17378-82-4; DNase, 9003-98-9.

References

Calladine, C. R. (1982) *J. Mol. Biol. 161*, 343–352.

Cartwright, I. L., & Elgin, S. C. R. (1982) *Nucleic Acids Res. 10*, 5835–5852.

Chen, C. H. B. & Sigman, D. S. (1987) *Science 237*, 1197–1201.

Dickerson, R. E. (1983) *J. Mol. Biol. 166*, 419–441.

Drew, H. R., & Dickerson, R. E. (1981a) *J. Mol. Biol. 151*, 535–556.

Drew, H. R., & Dickerson, R. E. (1981b) *J. Mol. Biol. 152*, 723–736.

Drew, H. R., & Travers, A. A. (1984) *Cell 37*, 491–502.

Flick, J. T., Eissenberg, J. C., & Elgin, S. C. R. (1986) *J. Mol. Biol. 190*, 619–633.

Gaynor, R. B., Kuwabara, M. D., Wu, F. K., Garcia, J. A., Harrich, D., Briskin, M., Wall, R., & Sigman, D. S. (1988) *Proc. Natl. Acad. Sci. U.S.A. 85*, 9406–9410.

Goyne, T. E., & Sigman, D. S. (1987) *J. Am. Chem. Soc. 109*, 2846–2848.

Klug, A., Jack, A., Kennard, O., Shakked, Z., & Steitz, T. A. (1979) *J. Mol. Biol. 131*, 669–680.

Kuwabara, M. D., & Sigman D. S. (1987) *Biochemistry 26*, 7234–7238.

Kuwabara, M., Yoon, C., Goyne, T. E., Thederahn, T., & Sigman, D. S. (1986) *Biochemistry 25*, 7401–7408.

Law, R., Kuwabara, M. D., Briskin, M., Fasel, N., Hermanson, G., Sigman, D. S., & Wall, R. (1987) *Proc. Natl. Acad. Sci. U.S.A. 84*, 9160–9164.

Maxam, A. M., & Gilbert, W. (1980) *Methods Enzymol. 65*, 499–599.

Nabel, G., & Baltimore, D. (1987) *Nature 326*, 711–713.

Pope, L. M., Reich, K. A., Graham, D. R., & Sigman, D. S. (1982) *J. Biol. Chem. 257*, 12121–12128.

Scheffler, I. E., Elson, E. L., & Baldwin, R. L, (1968) *J. Mol. Biol. 36*, 291–304.

Sen, R., & Baltimore, D. (1986) *Cell 46*.

Sen, R., & Baltimore, D. (1987) *Cell, 47*, 921–928.

Sigman, D. S. (1986) *Acc. Chem. Res. 19*, 180–186.

Sigman, D. S., Graham, D. R., D'Aurora, V., & Stern, A. M. (1979) *J. Biol. Chem. 254*, 12269–12272.

Sigman, D. S., Spassky, A., Rimsky, S., & Buc, H. (1985) *Biopolymers 24*, 183–197.

Spassky, A., & Sigman, D. S. (1985) *Biochemistry 24*, 8050–8056.

Spassky, A., Rimsky, S., Buc, H., & Busby, S. (1988) *EMBO J. 7*, 1871–1879.

Suggs, J. W., & Wagner, R. W. (1986) *Nucleic Acids Res. 14*, 3703–3716.

Thederahn, T. B., Kuwabara, M. D., Larsen, T. A., & Sigman, D. S. (1989) *J. Am. Chem. Soc. 111*, 4941–4946.

Veal, J. M., & Rill, R. L. (1988) *Biochemistry 27*, 1822–1827.

Veal, J. M., & Rill, R. L. (1989) *Biochemistry 28*, 3243–3250.

Yoon, C., Kuwabara, M. D., Law, R., Wall, R., & Sigman, D. S. (1988a) *J. Biol. Chem. 263*, 8458–8463.

Yoon, C., Prive, G. G., Goodsell, D. S., & Dickerson, R. E. (1988b) *Proc. Natl. Acad. Sci. U.S.A. 85*, 6332–6336.